On the role of thermal exposure on the stress controlled fatigue behavior Of an intermediate strength γ−TiAl based alloy

Huang, Ze; Huang, S.

DOI:
10.1016/j.msea.2015.03.091

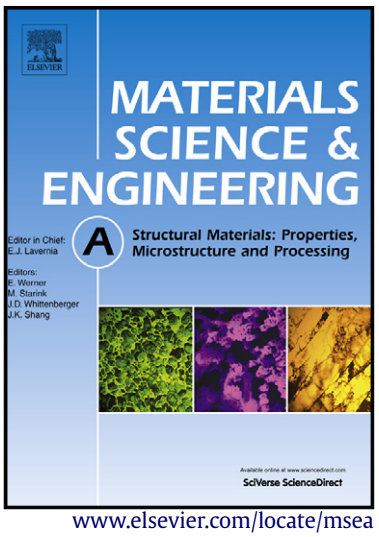

www.elsevier.com/locate/msea

On the role of thermal exposure on the stress controlled fatigue behavior Of an intermediate strength γ – TiAl based alloy

Z.W. Huang, S. Huang

PII: S0921-5093(15)00342-1
DOI: http://dx.doi.org/10.1016/j.msea.2015.03.091
Reference: MSA32188

To appear in: *Materials Science & Engineering A*

Received date: 18 February 2015
Revised date: 20 March 2015
Accepted date: 21 March 2015

Cite this article as: Z.W. Huang, S. Huang, On the role of thermal exposure on the stress controlled fatigue behavior Of an intermediate strength γ – TiAl based alloy, *Materials Science & Engineering A*, http://dx.doi.org/10.1016/j.msea.2015.03.091

On the role of thermal exposure on the stress controlled fatigue behavior of an intermediate strength γ–TiAl based alloy

Z.W. Huang[a,b*] and S. Huang[a]

[a] School of Materials Science and Engineering, Southwest Jiaotong University, Chengdu, Sichuan, 610031, P.R. China

[b] School of Metallurgy and Materials, The University of Birmingham, Edgbaston, Birmingham B15 2TT, U.K.

∗Corresponding author, Tel: 44 121 414 3436
Email address: zewenhuang9@sohu.com

Fatigue specimens with four types of surface (EDM plane-sited and notched, shot peened and electropolished) were assessed under three exposure conditions (no exposure, block exposure, individual exposure-oxidation at 700°C for 10000 h) to quantify the effects of surface roughness, stress concentration, oxidation and inner microstructural changes on fatigue strength of an intermediate strength TiAl alloy Ti-45Al-2Mn-2Nb-0.8vol%TiB_2. With $\sigma_{0.2}$=468MPa, S-N fatigue is found to be conducted mainly under a loading condition of $\sigma_{max} > \sigma_{0.2}$. Local plastic deformation occurred on the maximum-stressed surface. The alloy becomes less sensitive than high strength alloys ($\sigma_{0.2} >$ 600MPa) to surface damages and notches. Also observed is that electropolishing is less effective than shot peeing in improving the fatigue strength because the latter is able to produce a deep compressive-stress zone. The fatigue performances of all types of surface are improved when subjected to block exposure, attributed to thermal conditioning of the bulk material which is little changed during 10000-h exposure. Exposure-induced fatigue strengthening occurs on the EDM and electropolished surfaces but not on shot peened surface after individual exposure-oxidation. The fatigue behaviour of a specific surface depends upon whether or not the beneficial effects outweigh the detrimental effects, which are varied with varied surface. Also found is that electropolishing rather than shot peening is more effective in retaining oxidation resistance when subjected to long-term exposure-oxidation.

Key words: Gamma titanium aluminides; Thermodynamic stability; High cycle fatigue; Surface damage; Notch sensitivity; Scanning electron microscopy

1. Introduction

γ-TiAl based intermetallic alloys exhibit much steeper fatigue crack growth resistance curves and lower fracture toughness than conventional Ti-based and Ni-based alloys. A relatively narrow interval between the threshold stress intensity factor range ΔK_{th} and the maximum stress intensity factor K_{max} at final failure is often produced [1-6]. The fraction of total fatigue life resulting from crack propagation is therefore significantly small, and the total life is likely to be dominated by the number of cycles to crack initiation. Such characteristic features reveal the problems of defining a safe life for this type of materials. One approach to a reliable prediction of save-life for γ-TiAl alloys is to use conventional S-N fatigue curves. Fatigue strength, as a representative of fatigue crack initiation resistance, is considered to be one of the primary design drivers for TiAl alloys [7-9].

However, difficulties may still arise because steep crack growth resistance curves usually result in relatively flat S-N curves. A small increase in stress due to existence of stress raisers on sample surface could change the fatigue lifetime from essentially infinite to less than 10^5 cycles [10-12]. In view of the high sensitivity to surface quality for TiAl alloys, there is a need to develop a clear understanding of how surface defects and other stress concentrators, caused by component design, manufacturing and machining, impact of foreign object and surface oxidation, affect total life of γ–TiAl alloys under cyclic loading. Considerable amounts of research have been carried out to quantify the effects of surface quality [10, 13-16], notch [10, 17-19], foreign object damage [19-21] and oxidation layers [22, 23] on fatigue life of TiAl alloys. However, no much effort in this area has been made for γ-TiAl alloys which are subjected to a long-term thermal exposure in air. A γ-TiAl component in service is in fact exposed to elevated temperatures (say 700°C) in air environment for long

time (say 10000 hours). Three major types of microstrcural/micromechanical changes are expected to occur: (a) internal microstructual changes due to constituent dissolution, decomposition and phase transformation, (b) surface layer oxidation and (c) changes in suface defects and bulk stress concentration because of long-term exposure in a thermal enviroment. Therefore, it is necessary to assess all these effects on total life under the condition of long-term thermal exposure in air.

The present study concentrates on all these effects on the total life of an intermediate strength near lamellar γ-TiAl alloy. The alloy is to be studied under three thermal exposure schemes: a) no exposure, b) block exposure with internal changes but no surface oxidation, c) thermal exposure with both internal changes and surface oxidation. The objective of the study is to reveal how and to what extent the varied surface and bulk conditions under the three thermal exposure schemes affect the fatigue crack initiation resistence for an intermediate strength γ-TiAl based alloy. This work is expected to provide a reference guide for safe application of this type of TiAl alloys at elevated temperatures.

2. Experimental

The γ-TiAl based alloy in this study is a grain refined, intermediate strength ($\sigma_{0.2}$= 486 MPa) near lamellar alloy Ti-45Al-2Mn-2Nb (at. %)-0.8TiB_2 (vol. %), referred to as alloy 4522-0.8. The alloy ingot (96 mm in diameter) was produced using a double-melted PACH (Plasma Arc Cold Hearth) process. The ingot was hot isostatically pressed (HIPped) at 1260°C under a pressure of 150 MPa for 4 h, followed by an stabilizing treatment at 900°C for 24 h. The actual composition is very close to the nominal composition with an oxygen concentration of 650 wt ppm.

Three groups of specimens with three thermal exposure schemes were prepared: Group A, no exposure; Group B, exposure in block ingot without oxidation of individual specimens; Group C, individual specimen exposure with surface oxidation. Fatigue specimens of

dimensions 10 x 10 x 55 mm^3 were machined from HIPped and stabilised ingot. For every group four types of surface were prepared: EDM wire plane-sided and V-notched, shot-peened and electropolished. The details of the preparation procedures are listed in Table 1. A 60° V-shaped notch with a 0.20 mm root radius and 1.75 mm overall notch depth (K_t = 3，where K_t is the theoretical elastic stress concentration factor) was introduced. Notch was machined using one pass EDM wire, same as plane-sided EDM specimens. Shot peening was carried out after mechanical grinding of EDM wired samples, and performed by means of an injector type system using ϕ 0.4-0.5 mm sized zirconia-based ceramic spheres at an air-jet pressure of 5×10^5 Pa. The peening was done to achieve a full coverage of the maximum-stressed surface area. Electropolishing was carried out on mechanically ground and polished surface and performed at 20 volts in an electrolytic solution of 6% perchloric acid, 35% butanol and 59% methanol at - 25°C.

Surface roughness was measured using an Ambios XP-2 profilometer over a distance of 5 mm and represented in a standard Ra value. The Ra value in μm listed in Table 2 is an average of 5 measurements for each surface, with an error range assessed by standard deviation. For specimens in Group C, the surface roughness was measured on oxidised surface after individual exposure-oxidation. It can be seen from Table 2 that the EDM surface became slightly smoother but the shot peened and electropolished slightly rougher after oxidation than before. Microhardness profiles were measured to characterise the compressively strained surface after shot peening. The measurements were conducted on a HXD-1000TM Vickers micohardness tester with a load of 200 g.

After surface preparation, specimens in Group A were fatigue tested directly (named “no exposure”), and specimens in Group C were exposed individually in an air-circulated furnace at 700°C for 10000 h (named “individual exposure-oxidation”), then tested after exposure. In contrast to Group C, Group B was exposed as a 96 mm diameter ingot block (named “block exposure”) in the same furnace at 700°C for 10000 h. The exposed block was then machined

to testpieces, and prepared for the four types of surface. It appears that all specimens in Group B experience interior microstructural changes only, without surface oxidation.

S-N fatigue tests were carried out at room temperature in ambient air. Four point bending samples were tested on a PLG-100 electromagnetic resonance testing machine at a frequency of 100-125 Hz under a stress ratio R of 0.1 (where $R = \sigma_{min}/\sigma_{max}$, and σ_{min} and σ_{max} are the minimum and maximum stresses applied over the fatigue cycle respectively). The fatigue limit σ_{FL} is typically defined by the maximum stress σ_{max} at which a sample does not fail after 10^7 cycles ($\geqq 10^7$, called run-out).

The prepared surfaces and microstructures before and after thermal exposure were examined by scanning electron microscopy (SEM) using either secondary electron (SE) or backscattered electron (BSE) mode. Energy-dispersive X-ray spectroscopy (EDS) analysis was conducted on oxidized surface. The average colony size, obtained from more than 1000 colonies in SEM BSE images, was determined using linear interception method. The volume fraction and lath thickness of α_2 were measured on selected SEM BSE images using Image J software and checked by comparing them with measurements obtained from transmission electron microscopy (TEM). For all image analyses, mean values were determined with a standard deviation to represent the uncertainty of the measurements.

Results

3.1. The microstructure before exposure

The microstructure before exposure consists primarily of lamellar colonies, with small amounts of equiaxed γ (5.2±0.6 vol. %) and α_2 (1.5±0.2 vol. %) grains at colony boundaries (Fig. 1a). No retained β phase is observed since 4522-0.8 is a low β-stabiliser containing alloy. The lamellar colony size ranges from 22 to 228 μm, in which 90% of the colonies falls into a size range of 40-200 μm with an average size of 82.4±34.3 μm, determined from 965 lamellar colonies. The lamellar thicknesses and volume fraction of α_2 lamellae were

measured to be 0.49±0.22 μm and 20.6±3.7 vol. % before exposure, respectively.

3.2. The microstructural changes after exposure

The changes in bulk material induced by 10000 h exposure at 700°C were characterised in detail in a previous paper for this alloy [24]. A brief description is given here. The dominant change mode in lamellar colonies was that the α_2 lamellae thinned gradually and became more discontinuous after 10000 h exposure, as seen in Fig 1c and 1d. Some degree of parallel decomposition of thick α_2 lamellae into fine $\alpha_2+\gamma$ lamellae was observed. The average thickness of α_2 lamellae reduced to a half of the original value (0.25±0.14 μm) and the volume fraction of α_2 lamellae reduced by 1/4 after 10000 h exposure (15.0±5.5 vol.%). In contrast to the highly alloyed TiAl alloys investigated previously [25, 26], alloy 4522-0.8 showed no significant parallel decomposition of α_2 into fine $\alpha_2+\gamma$ lamellae, no perpendicular decomposition of α_2 into either $\alpha_2+\beta$ or $\alpha_2+\gamma$ sections and no formation (recrystallization) of β (B2+ω) grains on decomposed $\alpha_2+\gamma$ lamellae all through the exposure process. In fact, the low-alloyed alloy showed relatively restricted changes in microstructure and relatively stable mechanical properties after such a long-term exposure at 700°C.

3.3. The fatigue-specimen surfaces prepared before exposure

Fig. 2a shows the specimen surface produced by one-pass EDM wire. This appears to be a damaged surface consisting of widespread cavities (5-20 μm in size), protruded globes and ridges, and fine cracks (arrowed) due to local melting and electrical erosion induced. The surface roughness trace shows an average Ra=2.07 μm for one-pass EDM specimens (Table 2). Previous work from Trail and Bowen has found that a high level of tensile residual stresses (~300 MPa) was induced in the near-surface region after one-pass EDM wire of a low strength γ–TiAl based alloy ($\sigma_{0.1}$ = 310 MPa) [10]. The stresses were assumed to arise

mainly from the large thermal contraction of the liquid surface on the relatively cool base metal. Such tensile stresses may exceed the yield strength (even UTS) of the material, causing severe slip, twining and cleavage, depending on the crystal structure [27]. In the case of TiAl intermetallic alloy, such stresses cause cracking. Fig. 2b, a cross sectional view of the EDM surface, reveals that the surface cracks can run down to ~100 μm below the surface and the damaged surface is covered by a ~10 μm thick loose layer (indicated).

EDM surface was ground mechanically before shot peening. Shot peening of the ground EDM surface produced a heavy deformed surface with a number of shallow dimples, grooves and puckers (Figs. 3a and 3b). The surface roughness trace Ra reduced to 0.63 μm after shot peening which was 30% of the EDM value. Cross-sectional view of the peened specimen reveals that the deformed layer is about 80 μm in depth (Fig. 3b). This is significantly deeper than that produced in a high strength alloy under the same peening process [28]. It is generally accepted that materials with lower yield stresses are better able to absorb the impact of the shot particles by plastic deformation. The deformed layer is characterised by bending and kinking of the lamellae, in which α_2 lamellae are probably bent elastically. This is because α_2 phase is more significantly solution hardened and brittle than γ phase owing to its ability to scavenge interstitial impurities such as oxygen and carbon [29]. A survey of the shot peened surface shows that the bending of the lamellar structure is not uniform across the peened surface. The lamellae are barely deformed if they are arranged in lamellar packet consisting of very fine α_2-γ lamellae, as arrowed in Fig. 3c. Such lamellar packets look harder and stronger than individually distributed α_2-γ lamellae due to a size effect, thus more resisting to plastic deformation [30].

Also noted is that dynamic recrystallization and phase transformation occurred considerably in the deformed surface layer. As shown in Figs. 3c and 3d in BSE mode at a larger magnification, the conversion of microstructure due to deformation is characterised by dissolution of the α_2 lamellae and nucleation of small equiaxed grains in the γ lamellae.

Besides these microstructural changes, intense mechanical twining is observable in the γ lamellae and dislocations glide may also activate in untwining regions, inducing strong strain contrast. However, such a conversion of deformed microstructure is not observed in the surface regions where α_2 lamellae are arranged alternately with very fine γ lamellae (nanometer sized) in a packet fashion, such as those shown in Figs 3c. It is tempting to speculate that the avoiding of microstructural conversion could be related to a higher degree of elastic deformation, which was caused again by a size effect.

Fig. 4 shows the microhardness profiles in near-surface regions for the shot peened surfaces under the three thermal exposure conditions. As a result of the process-induced deformation, a hardened layer with compressive stress was produced in the subsurface region. It can be seen that the specimens without exposure (Group A) and with block exposure (Group B) show a ~ 300 μm-deep hardened region with a microhardness value at the surface 240 HV0.2 higher than the bulk values (300 HV0.2), indicating a 80 % increase in hardness for the two groups. The similarity in compressive stressed and hardened layer for Group A and B is understandable since the samples in Group B were EDM machined to shape after block exposure, and then shot peened. A significant decrease in hardness was observed in individual exposure-oxidation surface, which will be described in the following section.

Fig. 5a shows the elecropolished surface before exposure. The major constituents of the alloy can be observed clearly under BSE mode. The surface roughness trace was measured to be 0.22 μm after elecropolishing which was reduced to only 1/3 of the shot-peened value and 1/10 of the EDM value. The grinding and polishing plus electropolishing procedure used in this study is found to be able to take off a ~150-200 μm thick surface layer, which is sufficient to remove the whole EDM-produced damaged surface layer and even a thin layer underneath it, leaving an almost defect free surface prior to fatigue (Fig. 5b).

3.4. The fatigue-specimen surfaces after exposure and oxidation

There is no need to show all the four types of surface in Group B since they are very similar in morphology to their counterparts in Group A, based on the preparation procedure (section 2). This section focuses on the characteristic features of the four surfaces in Group C only, which demonstrates the effects of long-term oxidation on the prepared surfaces.

Figs. 6a and 6b show the normal and cross-sectional view of the oxidised EDM surface. The numerous holes, globes and cracks formed on EDM surface are now covered by an oxidation scale, and the surface looks still rough, see Fig. 6a. The surface roughness trace Ra changed to 1.82 μm. The value is not worse than the original EDM value (2.07 μm) without oxidation, indicating that the long-term oxidation process may not exacerbate the EDM wired surface roughness. The outmost loose scale consisting of fine and coarse oxides showed a breakaway morphology, indicating that severe spallation occurred on the specimen surface. Some part of the loose layer shown in Fig. 6b suggests the layer may range from 10-15 μm thick (arrowed in Fig. 6b). XRD analysis confirmed that the loose scale consisted of TiO_2-Al_2O_3 oxides [31], which was in consistence with the results obtained previously for other 2Mn-2Nb containing TiAl alloys [32, 33]. A featureless but relatively solid layer with varied thickness formed just below the oxidised loose layer. Fig. 6c, a BSE image of the middle part of Fig. 6b at a larger magnification, shows that this layer formed at the expense of α_2+γ lamellae. It looks like that the α_2 lamellae at surface were well dissolved and mixed with γ phase through diffusion during the long-term exposure-oxidation. The featureless layer is called diffusion layer in this paper. From Fig. 6c, it is clear that the dissolution and subsequent homogenization in the diffusion layer were not total completed after the 10000-h process. The BSE image clearly reveals a varied atomic number contrast across the diffusion layer, where no recrystallised γ grains can be found. Some cracks appeared within this layer, which could be original EDM cracks and/or an outcome of oxidation, which increased brittleness of the diffusion layer owing to formation of fine oxides inside the layer.

The oxidised surface of shot peened specimen is shown in Fig. 7. Spherical oxidised

particles formed unevenly on the heavily deformed surface (Fig. 7a). The surface roughness trace Ra after oxidation is 0.67 μm, which is similar to the value 0.63 μm obtained without oxidation (Table 2). Again, the long-term oxidation seems not to bring about surface degradation in terms of the Ra value. Cross-sectional view of the oxidised surface under BSE mode has found that the oxidation scale in fact is composed of three layers. They are, from outside towards inside, a loose layer with a breakaway morphology and a dark atomic contrast, a grey layer and a white layer. Between the layer structure and bulk material is a diffusion layer characterised by recrystallised γ grains. The outmost loose layer is thinner in shot peened specimen than in its EDM counterpart, which is 5-10 μm in depth (arrowed in Fig. 7b). The three layer structure of the oxidised scale can be viewed more clearly in Fig. 7c, a BSE image at a larger magnification. As shown in Fig. 7c, both white and grey layers are observed to be narrow in thickness and roughly continuous along the surface profile. The loose layer at outmost surface is a mixture of TiO_2-Al_2O_3 oxides, which are porous and easy to collapse through spallation. As demonstrated by EDS analysis results in Fig. 8, the white layer with strong atomic number contrast (point 1) is Mn-Nb enriched and Al-Ti depleted; and contains a small amount of oxygen. It indicates that during oxidation heavier metals Mn, Nb and Ti which partitioned originally in α_2 lamellae would be released by α_2 dissolution and diffuse towards the surface. Ti and Al were used to form TiO_2-Al_2O_3 oxides but Mn and Nb were accumulated to form a white layer at surface. They might form Mn-, Nb-containing oxides or even precipitated to form small sized α_2 and B2 (with ω) phases [34]. Between this bright layer and the loose dark layer is a narrow grey layer, which could be a transition region between the Al-Ti-O rich loose layer and Mn-Nb rich white layer. More important finding for the shot peened surface is that a diffusion layer consisting of equiaxed γ grains forms just below the white layer and above the bulk lamellar structure. As indicated by arrows in Fig. 7c, the layer of the equiaxed γ grains shows varied thickness, in a range of 10-20 μm. The formation of equiaxed γ grains means that 1) an Al-rich sub-surface region was formed below the Mn-Nb enriched white layer; 2) an energy-induced recrystallisation occurred as the

composition approached by diffusion. Such recrystallization resulted in relaxation of the deformation energy introduced originally by shot peening.

After individual exposure-oxidation in 700°C for 10000 h, the hardening effect of shot peened specimens was reduced significantly in Group C. The width of the hardening region seems not reduced but the hardening value is reduced significantly. Compared with the bulk value, the hardness increase at surface due to shot peening was reduced from 540 to 340 HV0.2 at surface and to 400 HV0.2 in the subsurface region (~100 μm inside), see Fig. 4. The surface due to shot peening is now only 13% harder at surface and 33% harder in the subsurface region relative to the bulk material. Thermal relaxation of surface hardening is a widely observed phenomenon [16, 28]. It should be related to the recovery of dense deformation structure. Moreover, recrystallisation in the heavily deformed layer is also expected to reduce the surface hardness since compressive strain is relieved with recrystallisation. The less reduction in hardness in subsurface region from inner 100 μm to 300 μm is of particular interest. This phenomenon was not observed in a high strength TiAl alloy which was subjected to the same shot peening process [28]. This indicates that the ability to retain work hardening of shot peening can be improved by forming a thicker deformation zone in materials with lower yield stresses. It is believed that with such a thicker and more intensively deformed subsurface region, the deformation-induced dislocation/twin structure cannot be annealed out easily so that microhardness and compressive stress could be left to some degree in the subsurface region. As shown in the bottom of Fig. 7c, such densely arranged twins are observable just below the diffusion (recrystallised) region.

The elecropolished smooth surface is covered evenly by loose scale after 10000 h exposure-oxidation at 700°C in air (Fig. 9a). The oxidised scale makes the surface less smooth, the roughness value Ra is reduced from 0.22 μm to 0.31 μm after exposure-oxidation. Cross sectional observation of the oxidised surface in Fig. 9b has found that the outmost loose layer is similar to its shot-peening counterpart in thickness (5-10 μm) but thinner than

EDM. No noticeable oxidation pegs and internal oxides were observed. Detailed observation in Fig. 8c under BSE mode reveals that the oxide scale consists of semi-continuous grey and white layers just below the loose layer. However, both the layer are thinner and less continuous than those observed at shot peened surface, suggesting that the diffusion of the heavier metals towards the surface is less active in the electropolished specimen. Without formation of a thicker and more continuous oxidized layer structure at the surface, coarsened α_2 lath sections formed in the near surface region with dissolution of α_2 lamellae below it. This indicates clearly that the oxidation process proceeded on the electropolished surface more slowly than on the shot peened and EDM surface. Also observed is that some equiaxed γ grains formed in the α_2 lamellae dissolution region. But the formation of such grains is not as significant as found in shot peened surface since no intense plastic deformation and compressive stress exist as driving force for recrystallization.

3.5.The stress-fatigue behavior of Group A specimens

Fig. 10a through 10c shows the S-N fatigue performance of the four types of surface for each exposure groups. Fig. 11a through 11d summarises the S-N fatigue performance of the three exposure groups for each surface. Fatigue strength data are listed and analysed in Table 3 for the three types of plane-sited surface and in Table 4 for V-notch specimens. All the percentage data listed in Table 3 and 4 are approximated to the nearest integer.

As seen in Fig. 10a and Table 3, the run out occurred when σ_{max} = 380 MPa (i.e. σ_{FL} = 380MPa) for EDM wired surface before exposure. The 0.2% proof stress and UTS for alloy 4522-0.8 is 486 MPa and 524 MPa, giving a ratio $\sigma_{FL}/\sigma_{0.2}$=0.78 and σ_{FL}/σ_{UTS}=0.73, respectively. Higher ratios, close to 1 or even bigger than 1 were obtained for enhanced surfaces (Table 3). These ratios are significantly higher than those obtained in a high strength TiAl alloy where the same EDM wired surface showed a ratio $\sigma_{FL}/\sigma_{0.2}$ = 0.45 and σ_{FL}/σ_{UTS} = 0.42 [28]. This means that the degradation in fatigue resistance owing to severely surface

damage can become moderate with reduced yield strength. A previous study has found that further reduction of yield strength for one pass EDM surface can make the $\sigma_{FL}/\sigma_{0.2}$ ratio even greater than 1 [10]. It is therefore evident that the loss in fatigue limit caused by the same EDM process is related to the alloy strength. With reduced alloy strength, the fatigue behaviour can become less sensitive to the damaged surfaces.

Shot peening of EDM surface improves fatigue strength significantly, σ_{FL} increased from 380MPa to 550MPa, increased by 45% before exposure. This result is consistent with the hardened condition produced. As described in section 3.3, highly intense deformation was produced in the subsurface region, which not only removed the widespread surface defects but also produced a compressively stressed layer with significant hardening (hardened by 80%) in the outer 300 μm of the specimens.

On the other hand, electropolishing (after mechanical grinding and polishing) of the EDM surface resulted in a considerably lower improvement in fatigue strength, σ_{FL} = 480MPa, increased by 26% relative to 45% increase by shot peening. The comparison is of particular interest because it is in contrast to the performances recorded for a high strength TiAl alloy (alloy 4Nb-4Zr) for which almost the same shot peened and electropolished processes were employed. For alloy 4Nb-4Zr ($\sigma_{0.1}$ = 621 MPa), the increase in σ_{FL} was 36% by shot peening and 68% by electropoling [28]. A similar result, in which the electropolished surface outperforms the shot peened surface, was reported for another high strength ($\sigma_{0.2}$ = 625 MPa) TiAl alloy [15]. It tends to suggest that alloy strength matters in terms of which surface is more effective in improving fatigue behaviour. The surface produced by electropolishing can outperform the shot peened surface if the yield stress is high enough but the reverse would be obtained if the yield stress is reduced to a certain level.

S-N data for a V notch fatigue tests are presented using net section in Table 4. As would be expected, the fatigue limit σ_{FL} reduced significantly: from 380 MPa in plane-sided specimens to 146 MPa. A fatigue notch factor K_f = 2.60 and a ratio of K_f/K_t = 0.87 is obtained for

non-exposure condition. K_f is the notch factor used to express the effectiveness of the notch in decreasing $\sigma_{FL,}$ while K_t is the theoretical elastic stress concentration factor. Here, K_f is calculated based on σ_p/σ_n (σ_p and σ_n are the fatigue limit at run out for plane-sided and notched specimens, respectively). It is generally recognised that if K_f is not close to the K_t, the material is regarded as less sensitive to the notch. The present ratio K_f/K_t is 0.87 in Group A, which is slightly lower than that ($K_f/K_t = 0.93$) obtained for high strength alloy 4Nb-4Zr, indicating a slightly reduced notch sensitivity. The notch sensitivity can also be represented by notch sensitivity factor Q ($Q = K_f\text{-}1/K_t\text{-}1$). As seen in Table 4, Q is 0.8 for Group A, which is not very close to the extreme value 1 for the non-exposed alloy 4522-0.8, indicating again a reduced notch sensitivity factor for the intermediate strength TiAl alloy.

3.6. The stress-fatigue behavior of Group B specimens

As shown in Fig. 11, every type of the surface in Group B after block exposure has the fatigue performance superior to its counterpart in Group A. The specific increases in σ_{FL} relative to Group A are listed in Tables 3 and 4. A marginal increase (5%) is obtained for EDM surface, a noticeable increase (15%) for the shot peened and a remarkable increase (28%) for the electropolished. Moreover, the fatigue limit σ_{FL} increases from 146 MPa before exposure to 200 MPa after block exposure for V-notch specimens, about 1/3 increase (37%). All the results indicate clearly that block exposure of alloy 4522-0.8 at 700°C for 10000 h is beneficial to fatigue performance. The enhanced fatigue behaviour is believed to come from stress relaxation and microstructural consolidation of the bulk material when immersed into a warm-air (700°C) environment for 10000 h. Such a stress relaxation and microstructural consolidation can be regarded as "thermal conditioning" of the bulk alloy, of which main microstructural constituents were little changed during exposure.

For EDM wired surface, fatigue limit σ_{FL} increased from 380 MPa in no exposure condition (Group A) to 400 MPa in block exposure condition (Group B), increased by 5%. If

considering the uncertainty in S-N data often associated with TiAl alloys, it is reasonable to say that the fatigue performance hardly changed for the EDM specimens before and after exposure. This reflects the fact that fatigue cracks are relatively easy to initiate from the severely damaged surface layer, regardless of the stress relief and microstructure consolidation after block exposure.

However, higher degree of improvement in fatigue performance was obtained for shot peened and electrpolished specimens in Group B than in Group A. After block exposure, the fatigue strength at run out is 635 MPa for the shot peened and 615 MPa for the electropolished. If compared with EDM surface in the same group, the increase in σ_{FL} is 59% for shot peening and 54% for electropolishing in Group B while the increase in σ_{FL} is 45% for the former and 26% for the latter in Group A. Also noted is that the difference in fatigue performance between the two surfaces becomes significantly less after block exposure (20MPa) than before block exposure (70MPa). The increased similarity suggests that fatigue behaviour of the two surfaces is increasingly governed by the inner bulk material which has experienced the same thermal conditioning during block exposure.

The notch sensitivity is found to reduce significantly after long-term block exposure for the intermediate strength alloy. The notch sensitivity factor Q is only 0.5 and the ratio of K_f/K is 0.67 after block exposure. Both are far from the extreme value 1, indicating that the alloy after block exposure becomes less sensitive to the notch. The significant decrease in Q and K_f/K_t for the V notched in Group B is consistent with the fact that the peak cyclic stress always remains higher than the yield stress ($\sigma_{0.2}$ = 477MPa after exposure) for all the specimens in fatigue (see Fig. 10d). Under the loading condition of $\sigma_{max} > \sigma_{0.2}$ (here the σ_{max} at notch root is defined by taking into account of K_t), some degree of plastic deformation is expected to occur around the notch root and a certain degree of notch strengthening is produced as a result, giving rise to reduced notch sensitivity.

3.7.The stress-fatigue behavior of Group C specimens

Fig. 11 shows that the fatigue performances of the EDM wired (plane-sited and V-notched) and electropolished surfaces in Group C are improved after individual exposure-oxidation, compared with the three surfaces in Group A. This suggests that the harmful effect of oxidation at surface could be outweighed by thermal conditioning, involved in stress relaxation and microstructural consolidation when immersed in warm-air environment for long time. It is interesting to note from Table 3 and 4 that the improved fatigue strength in Group C over Group A is higher for EDM surface (32 % for plane-sited and 44% for V-notched) than for the electropolished (19%). This phenomenon is attributed to an extra beneficial effect acting on the EDM surface. When immersed into the warm air environment, the residual tensile stresses in the near surface layer of EDM samples are expected to relax and dissipate significantly, and the surface stress raisers such as eroded holes, protruded globes and microcracks could become less sensitive to cracking. From this reason, the EDM surface has shown a greater potential than electropolishing for fatigue improvement through individual exposure-oxidation and, the potential is reduced with improved surface quality.

Among the four types of surface, the shot peened is the only surface that shows a deteriorated fatigue strength, reduced to 510 MPa after individual exposure-oxidation, compared with 550MPa in Group A (no exposure) and 635MPa in Group B (exposure without oxidation). The reduction in σ_{FL} can be partially attributed to thermal relaxation of compressive stresses in the outer layer during the warm-air immersion. As shown in Fig. 4, the hardness was only 13% harder at surface and 33% harder in the subsurface region relative to the bulk material, while it was 80% harder than bulk alloy in Group A before exposure. Also noted is that the lamellar microstructure in surface layer during exposure-oxidation was changed to a layer of equiaxed γ grains through recrystallization, through which both plastic deformation and elastic deformation were alleviated considerably. Both of the changes are

considered to be negative to fatigue crack resistance. These, associated with negative effect of surface oxidation, are expected to outweigh the positive effect of inner stress relaxation and bulk material consolidation.

Respective comparison of the fatigue performance between Group C and Group B for all the four types of surface is able to differentiate the actual effect of oxidation from the effect of thermal conditioning of bulk material since both groups have experienced the same thermal exposure at 700°C for 10000 h. The exposure is expected to produce similar effect from bulk material, although there is a size difference: Group B was exposed in a large sized block while C in individual testpieces. The comparison between Group B and C has found that the EDM wired surface, no matter plane-sited or notched, is the only surface that has shown improved fatigue strength after oxidation, increased by 25% (Table 3). This is unexpected since thickest oxidation scale was formed at the EDM surface among the group. On the other hand, as would be expected, oxidation has reduced the fatigue strength both for shot peened and for electropolished specimens: 20 % reduction for the former and 7% for the latter (Table 3) relative to the non-oxidised surface in Group B. The higher degree of degradation on shot peened surface than on electropolihed surface was also observed in other TiAl alloys with varied yield strengths [35]. It is reasonable to assume that the surface roughness is a key factor against oxidation at 700°C. With a much reduced surface roughness of 0.22 μm produced by electropolishing, the ability to maintain a relatively consistent fatigue behaviour is above that with a roughness of 0.63 μm produced by shot peening. Also understandable is that the intense plastic deformation and compressive residual stress in the hardened layer produced by shot stream was found to reduce significantly during the thermal process (Fig. 4), which should be responsible for the higher degree of degradation.

It can be seen from Fig. 10c that after a long-term individual exposure-oxidation, the three types of plane-sided surface in Group C end up having increasingly similar fatigue behaviour than in other two groups. As shown in Table 3, the positive contribution of shot

peening to fatigue strength over EDM reduced from 45% in Group A and 59% in Group B to only 2 % in Group C. The improvement in fatigue strength by electropolishing over EDM reduced from 26% in Group A and 54 % in Group B to 14 % in Group C. It appears that the two surface improvement procedures applied for alloy 4522-0.8 become less effective in raising fatigue resistance after individual exposure-oxidation. In contrast to the two surfaces, EDM wired surface shows that the detrimental effect of damaged surface on fatigue performance is alleviated by such a long-term warm air immersion, giving rise to a 32% increase after individual exposure-oxidation.

Discussion

4.1. Effect of surface type on fatigue strength

Pre-yielding crack initiation is easy to occur on EDM surface because of a damaged surface, no matter whether the σ_{max} applied is below or above the yield strength. As analysed by Trail and Bowen, a high level of tensile residual stresses was introduced to the surface and subsurface layer by one pass EDM wire [10]. The stresses presumably arose from localised melting, rapid solidification and thermal contraction owing to strong electric current involved. When superimposed on the applied fatigue stresses, the residual tensile stresses are expected to effectively increase the mean stress of the fatigue cycle and decrease the fatigue life for crack initiation. Under the worst condition, no crack nucleation stage is needed. EDM specimens may directly enter a crack initiation stage if the maximum stress on the surface layer is higher than the threshold value for crack initiation.

Introduction of a V-notch to RDM surface has caused stress concentration at the notch root where the volume of material sampled by the local peak stress is much small. The notched specimens, as would be expected, show decreased fatigue limit, but not to the extent that the theoretical K_t value of the V-notch would have predicted. The present results, fatigue notch factor $K_f = 2.6$ and notch sensitivity factor $Q = 0.8$, indicate that the alloy 4522-0.8 is

not as sensitive to V-notch as the high strength alloy 4Nb-4Zr which has a K_f = 2.8 and Q = 0.9. This comparison clearly reveals that decreasing the yield strength can reduce notch sensitivity. With a certain extent of decrease in yield strength, V notched specimens would be tested under loading condition of $\sigma_{max} > \sigma_{0.2}$. Under such a loading condition, considerable plastic deformation is expected to occur at notch root, which results in a certain degree of "notch strengthening". Notch strengthening behaviour can be well understood by looking into the microstructural features in the vicinity of notch root. Fractographic examination on the fracture surface of a V-notched sample (σ_{max} = 176 MPa, failed at $N_f = 5x10^5$ cycles) has recorded noticeable plastic deformation in the near root region (Fig. 12a). Plastic deformation of lamellar colonies was normally characterised either by geometrically arranged parallel steps or by delaminated big facets which are orientated to a certain angle to the tensile axis so that a large Schimid factor is involved [36, 37].

Improving the surface quality is sure to increase the fatigue performance for alloy 4522-0.8. However, on comparison of the degree to which the fatigue strength is increased between intermediate strength alloy 4522-0.8 and high strength alloy Ti-44Al-4Nb-4Zr, it is found that a higher degree of improvement is achieved by alloy 4522-0.8 through shot peening (45% by 4522-0.8 vs 36% by 4Nb-4Zr) but a higher degree of improvement is achieved by alloy 4Nb-4Zr through electropolishing (68% by 4Nb-4Zr vs 26% by 4522-0.8). It appears that the surface prepared by shot peening outperforms the surface prepared by electropolishing if the yield stress is moderate. The critic factor behind this is considered to be the degree of deformation and hardening in the surface-subsurface layer caused by shot stream. With a moderate strength of $\sigma_{0.2}$=486 MPa, a more intense and deeper penetrating plastic deformation is induced in alloy 4522-0.8 than in alloy 4Nb-4Zr when the same shot peening was performed. Consequently, a deeper compressive-stress zone and a higher resistance to crack initiation are achieved for the less strengthened alloy. Fig 12b reveals some degree of plastic deformation, characterized by parallel geometric steps inside lamellae,

occurred near the maximum-stressed shot peened surface. On the other hand, the surface produced by electropolishing outperforms the shot peened if the yield strength is high. The critic factor behind this is considered to be whether the specimens are tested under a loading condition of $\sigma_{max} < \sigma_{0.2}$ or $\sigma_{max} > \sigma_{0.2}$. For a moderate alloy with the yield strength of $\sigma_{0.2}$ = 486 MPa like alloy 4522-0.8, a loading condition of $\sigma_{max} > \sigma_{0.2}$ applies for most of the electropolished specimens (Fig. 10a), plastic deformation through intense planar slipping and twining are likely to activate at maximum-stressed surfaces. The derivative microcracks are therefore relatively easy to nucleate, even on electropolished specimen with a defect-free surface. On the other hand, for a high strength alloy with yield strength $\sigma_{0.1}$ = 621 MPa like alloy 4Nb-4Zr, a loading condition of $\sigma_{max} < \sigma_{0.1}$ applies for all the electropolished specimens [28]. Plastic deformation through dislocation slipping and twining is difficult to activate at surface. Without intense plastic deformation, the surface quality becomes increasingly important for fatigue performance since a crack nucleation stage is needed before crack initiation. A defect-free surface therefore would have much enhanced fatigue performance, relative to defect containing surfaces.

4.2. Effect of block exposure on fatigue strength

The enhanced fatigue behaviour observed in Group B appears to be related to the characteristic changes of bulk material because all the surfaces in Group B are the same as its counterpart in Group A. As described in section 3.2, the alloy after 10000-h exposure at 700°C only demonstrated restrict changes in microstructure, characterized mainly by a gradual thinning of α_2 lamellae. There is no considerable oxygen-releasing embrittlement caused by significant dissolution of α_2 lamellae, no phase-transformation embrittlement caused by formation of B2+ω since no B2+ω phase in the low-alloyed alloy, and no other brittle particles precipitation such as silicides in this alloy. Consequently, the tensile properties were hardly changed [24]. Without considerable negative impacts from

microstructural embrittlement, the enhanced fatigue behaviour is deduced to be related to a "warm-air relaxation" phenomenon. Immersion of the block material in the warm air environment for 10000 h is expected to relax residual stresses and to consolidate the bulk microstructure through dissipating pile-up dislocations at interfaces, relieving segregation and stress concentration at grain boundaries, inactivating microcracks and other defects in the subsurface region. As a result, the bulk material under a long-term "thermal conditioning" somehow becomes more difficult to initiate and activate microcracks, leading to fatigue failure at increased stress levels.

A marginal increase of 5% in fatigue strength was recorded for EDM wired surface after block exposure. This indicates that the fatigue strength does not benefit considerably from block exposure if the surface is seriously impaired. This is because fatigue cracks are simply easy to initiate from the damaged surface, no matter how the stress relief and microstructure consolidation occurred in the inner region. In other words, with a significant impact from the damaged surface, the fatigue behavior would not be governed by inner bulk microstructure.

However, in the case of V-notch specimens, a significant increase of 37% in fatigue strength was recorded after block exposure. The controlling factors are assumed to be: 1) Fatigue of V-notch specimens after block exposure was conducted totally under the loading condition of $\sigma_{max} > \sigma_{0.2}$, which raised the stress level well above the yield stress of the alloy. More intense and higher degree of plastic deformation is expected in the immediate vicinity of the notch root, compared with those in Group A. Therefore, notch sensitivity factor Q was reduced accordingly from 0.8 to 0.5 and K_f/K ratio reduced from 0.87 to 0.67 after block exposure. 2) Relaxation of tensile residual stress and consolidation of bulk material during block exposure may play a role in reducing the notch sensitivity since both changes can reduce the probability of premature failure at notch root.

The present results from Group B reveal that as the detrimental effects from surface

defects are reduced either by surface hardening (shot peening) or by surface roughness reduction (electropolishing), fatigue crack initiation can be forced to shift to inner regions. The fatigue performance is therefore increasingly governed by inner microstructure of bulk material. With a little changed but long-term thermally conditioned bulk material, the number density of defects is expected to decrease, the degree of stress concentration is expected to decline and the resistance to crack initiation is expected to increase. All of these expectations were supported by the testing results: an increase in σ_{FL} by 15% for shot peening and by 28% for electropolishing was obtained in Group B when compared with Group A. The similarity (635 MPa vs 615MPa) in fatigue performance between the two surfaces also provides evidence to support the controlling effect of inner bulk material. Based on this effect, deterioration of inner microstructure of bulk material, on the other hand, is sure to result in degradation of fatigue performance, and a similarity in fatigue strength should be also observed for the two surfaces. It was found that this was the case in the high strength alloy 4Nb-4Zr, where a decrease in σ_{FL} by 8% for shot peening and by 28% for electropolishing were produced in Group B when compared with Group A, and the similar fatigue strength (350MPa vs 340MPa) for the two surfaces was also observed after block exposure [28].

4.3. Effect of individual exposure-oxidation on fatigue strength

Individual exposure-oxidation brings about two major changes to all specimens in Group C: 1) moderate microstructural changes and thermal conditioning of bulk material, 2) oxidation damage in surface layer. The former was observed to be beneficial to fatigue performance, but the latter appears to be harmful to the fatigue for all the four types of surface. Besides the two contradictory effects, warm-air environment has also altered, either beneficially or detrimentally, the original surface stress condition for EDM and shot peening surfaces. Therefore, no universal fatigue strengthening is observed for the four surfaces. The

specific fatigue behaviour in Group C can only be understood individually, depending upon whether or not the beneficial effects outweigh the detrimental effects for a specific surface.

It is surprising to find that the EDM surface, either plane-sited or notched, is the only surface showing the improved fatigue strength after individual exposure-oxidation, relative to Group A (increased by 32%) and Group B (by 25%). It seems that the formation of oxidized layer after 10000-h oxidation at 700°C is not harmful enough to bring down the fatigue resistance for the EDM wired alloy. By contrast, the worst EDM surface containing tensile stress and widespread defects has the highest potential for fatigue resistance improvement through individual exposure-oxidation. Explanations for such an unexpected increase are based on an extra beneficial effect: dissipation of surface tensile stress and inactivating surface defects when immersing individual specimens into a warm-air (700°C) environment for 10000 h. That is to say that the original damaging introduced by EDM process can be alleviated and inactivated by a warm-air environment. This, associated with the universal benefit from thermal conditioning of bulk material, outweighs the negative effect of surface oxidation, resulting in improved fatigue behaviour for EDM wired surfaces. Such a higher fatigue resistance obtained after oxidation (Group C) than before oxidation (Group A and B) has also been observed for quite a few γ–TiAl based alloys which were subjected to the same experimental scheme [28, 35].

For shot peened surface, on the other hand, the fatigue strength has been reduced to 510 MPa after individual exposure-oxidation, which is 7% lower than in Group A and 20% lower than in Group B. Explanations for such decreases are based on an extra detrimental effect resulted from weakening of the compressive stresses layer of shot peened specimen by individual exposure-oxidation, besides the two contradictory effects found on all types of surface in Group C. Long-term warm-air environment has softened the hardened surface to a certain degree through thermal relaxation of compressive stresses in the outer layer for the shot peened surface. One example of the thermal relaxations is represented by

recrystallization of a layer of equiaxed γ grains in the subsurface region. Such an extra negative effect has greatly impaired the ability to resist fatigue crack initiation for shot peening surface. This, associated with negative effect of surface oxidation, is expected to outweigh the positive effect of thermal conditioning of bulk material.

In the case of the electropolished surface, a complicated outcome is obtained after individual exposure-oxidation. The fatigue strength increased from 480 MPa in Group A to 615 MPa in Group B after block exposure, owing to thermal conditioning of bulk material. But the fatigue strength in turn reduced to 570 MPa when subjected to individual exposure-oxidation in Group C. The decrease of 45 MPa in σ_{FL}, relative to Group B, should be attributed to the surface oxidation. Such a decrease (7%) is relatively moderate compared with 20% decrease in the shot peened surface after the same exposure-oxidation. It is evident that the electropolishing surface outperforms the shot peening surface when individual exposure-oxidation is involved since the latter has suffered an extra detrimental effect, as mention above. The results tell us clearly that under our present experimental conditions electropolishing rather than shot peening is more effective in retaining the oxidation resistance for the alloy. It is therefore reasonable to deduce that the controlling factor against oxygen penetration at 700°C is the surface roughness rather than the highly-deformed and compressively-stressed surface layer since the latter has more structure defects. The deformation and compressive stress would be relaxed and dissipated in such a warm environment, while the "defect-free" surface is capable of maintaining the surface quality at a relatively high level.

Comparison of the fatigue strength for electropolishing surface between Group A (σ_{FL}= 480 MPa) and Group C (σ_{FL}= 570 MPa) is of particular implication: 19% increase (from 480MPa to 570MPa) in σ_{FL} is achieved even oxidation layer is formed. This improvement unambiguously provides evidence that oxidation has shown no worrying impact on electropolished alloy 4522-0.8 in terms of fatigue crack initiation resistance, provided the

bulk material is subjected to thoroughly thermal conditioning. This simply indicates that the beneficial effect of thermal conditioning through relaxation of residual stresses and consolidation of bulk microstructure outweighs the harmful effect of oxidation damage for the electropolished surface. An alternative comparison between 0-h exposure and 10000-h exposure can reveal the "exposure-induced fatigue strengthening" behaviour more clearly. Individual specimens for 10000-h exposure were EDM machined to shape, then exposed at 700°C for 10000 h and followed by electropolishing to prepare the same surface as those in Group A/B. That is to say, no oxidation layer is left after individual exposure. Without the detrimental effect of oxidation, the σ_{FL} after 10000h exposure at 700°C increased from 480 MPa to 620 MPa, increased by about 30%, as reported in a previous paper [24]. The result also indicates the size effect is trivial since the σ_{FL} (620MPa) from individual exposure is quite similar to that (615 MPa) from block exposure (Group B). It is interesting to find that the increase in σ_{FL} due to the 10000h exposure is roughly the same: about 30% for quite a few alloys studied [24-26, 28]. This simply indicates that the thermal conditioning of bulk material and the corresponding "exposure-induced fatigue strengthening" are essentially the same for all these alloys, provided they follow the same "machining→ exposure→surface preparation" procedure.

Conclusions

1. With an intermediate yield strength of $\sigma_{0.2}$ = 468MPa, alloy 4522-0.8 is less sensitive than high strength alloys ($\sigma_{0.2}$ > 600MPa) to surface damages, producing a ratio $\sigma_{FL}/\sigma_{0.2}$ =0.78 and σ_{FL}/σ_{UTS} =0.73 for EDM wired surface.

2. A V-notch sensitivity Q = 0.8 is obtained for the alloy before exposure and the factor can be even lower after exposure. Under loading condition of $\sigma_{max} > \sigma_{0.2,}$ some degree of plastic deformation and "notch strengthening" is produced at notch root.

3. With the intermediate yield strength, shot peening rather than electropolishing is more effective in increasing fatigue strength before exposure. A deeper penetrating plastic deformation and deeper compressive-stress zone can be produced. On the other hand, most of the electropolished specimens were tested under a loading condition of $\sigma_{max} > \sigma_{0.2}$. Microcracks were relatively easy to nucleate through plastic deformation on the maximum-stressed surfaces, even though they were nearly defect-free.

4. Fatigue performances are improved for all types of surface when subjected to block exposure, attributed to a long-term thermal conditioning of bulk material which is little changed during 10000-h exposure at 700°C.

5. Exposure-induced fatigue strengthening occurs on the EDM and electropolished surfaces but not on shot peened surface after individual exposure-oxidation. The specific fatigue behaviour can only be understood individually, depending upon whether or not the beneficial effects outweigh the detrimental effects for a specific surface.

6. Oxidation damage on electropolished surface has shown no worrying impact on fatigue crack initiation resistance for alloy 4522-0.8, provided the bulk material is subjected to thoroughly thermal conditioning. Also found is that electropolishing with a much reduced surface roughness rather than shot peening with hardened surface is more effective in retaining oxidation resistance for the alloy.

Acknowledgement

The authors gratefully acknowledge the National Natural Science Foundation of China for financial support (Project number: 51271154). The authors thank Mr. Hong Liang Sun for some management help during this work. ZWH is also very thankful to the School of Metallurgy and Materials, The University of Birmingham, U. K. for some experimental support.

References

[1]. A.W. James, P. Bowen, Mater Sci Eng A 153 (1992) 486-492.

[2]. W.O. Soboyejo, K.T. Venkateswara Rao, S.M.L. Sastry, R.O. Richie, Metall Trans A 24 (1993) 585-600.

[3]. D.L. Davidson, J.B. Campbell, Metall Trans A 24 (1993) 1555-1574.

[4]. P Bowen, R.A. Chave, A.W. James, Mater. Sci. Eng A 192/193 (1995) 443-456,

[5]. K.T. Venkateswara Rao, Y-W. Kim, C.L. Muhlstein, R.O. Richie, Mater Sci Eng A 192/193(1995) 474-482.

[6]. Z.W. Huang, P. Bowen, in: X.R. Wu, Z.G. Wang (Eds.), Fatigue'99, 7th Intl. Fatigue Congress, HEP & Emas, Beijing, 1999, vol. III, pp. 1585-1590.

[7]. J.M. Larsen, B.D. Worth, S.J. Balsone, J.W. Jones, in: Y-W. Kim, R. Wagner, M. Yamaguchi (Eds.), Gamma Titanium Aluminides, TMS, Warrendale, PA, 1995, pp. 821-834.

[8]. R.O. Ritchie, in: X.R. Wu, Z.G. Wang (Eds.), Fatigue'99, 7th Intl. Fatigue Congress, HEP & Emas, Beijing, 1999, vol. I, pp. 3-14.

[9]. J.M. Larsen, A.H. Rosenberger, B.D. Worth, K.Z. Li, D.C. Maxwell, W.J. Porter, in Y-W. Kim, D.M. Dimiduk, M.H. Lorreto (Eds.), Gamma Titanium Aluminides, TMS Warrendale, PA, 1999, pp. 463-472.

[10]. S.J. Trail, P. Bowen, Mater Sci Eng A 192/193 (1995) 427-434.

[11]. G. Henaff, A-L Gloanec, Intermetallics 13 (2005) 543-558.

[12]. S.K. Jha, J.M. Larsen, A.H. Rosenberger, Acta Mater 53 (2005) 1293–1304.

[13]. P.E. Jones, D. Eylon, Mater Sci Eng A 263 (1999) 296–304.

[14]. A.R.C. Sharman, D.K. Aspinwall, R.C. Dewes, P. Bowen, Wear 249 (2001) 473–481.

[15]. X. Wu, D. Hu, M. Preuss, P.J. Withers, M.H. Loretto, Intermetallics 12(2004) 281–287.

[16]. J. Lindemann, C. Buque, F. Appel, Acta Mater 54 (2006) 1155–1164.

[17]. M. Nazmy, M. Staubli, G. Onofrio, V. Lubinc, Scripta Mater 45 (2001) 787-792.

[18]. M. Filippinia, S. Beretta, L. Patriarca, G. Pasquero, S. Sabbadini, Procedia Engineering 10 (2011) 3677–3682.

[19]. W.E. Voice, M. Henderson, E.F.J. Shelton, X. Wu, Intermetallics 13 (2005) 959–964.

[20]. T.S. Harding, J.W. Jones, P.S. Steif, T.M. Pollock, Scripta Mater 40 (1999) 445–449

[21]. M.R. Bache, C.C. Morgans, Intermetallics 19 (2011) 782-786.

[22]. S.K. Planck, A.H. Rosenberger, Mater Sci Eng A 325 (2002) 270–280.

[23]. A. Zeller, F. Dettenwanger, M. Schutze, Intermetallics 10 (2002) 33–57.

[24]. Z.W. Huang, W. Hu, Intermetallics 54 (2014) 49-55.

[25]. Z.W. Huang, Intermetallics 37 (2013) 11-21.

[26]. Z.W. Huang, Intermetallics 42 (2013) 170-179.

[27]. H.K. Lloyd, R.H. Warren, J. Iron Steel Inst, 203 (1965) 238-247.

[28]. Z.W. Huang, C, Sun, Mater Sci Eng A 615 (2014) 29-41.

[29]. A. Denquin, S. Naka, A. Huguet, A. Menand, Scripta Metall Mater 28 (1993) 1131-1136.

[30]. L. Cha, C. Scheu, H. Clemens, H.F. Chladil, G. Dehm, R. Gerling, A. Bartels, Intermetallics 16 (2008) 868–875.

[31]. S. Huang, Mater degree thesis “Study of surface microcrack initiation, fatigue life and oxidation behaviour for a long-term thermal-exposed γ-TiAl alloy Ti-45Al-2Mn-2Nb-0.8vol%TiB2”, Southwest Jiaotong University, China, 2013. Classified Index: TG111.8.

[32]. V.A.C. Haanappel, M.F. Stroosnijder, Surface and Coatings Technology 105 (1998) 147–154.

[33]. A.R. Rastkar, B. Shokri, T. Bell，Surface and Coatings Technology 202 (2008) 6038–6048.

[34]. U. Prasad, Q. Xu, M.C. Chaturvedi, A.K. Jena, Intermetallics 8 (2000) 125-131.

[35]. Z.W. Huang, unpublished results, 2015.

[36]. Z.W. Huang, P. Bowen, Acta Mater 47 (1999) 3189–3203.

[37]. Z.W. Huang, P. Bowen, I.P. Jones, Philosophical Mag A 81 (2001) 2183–2197.

Captions

Fig. 1 SEM BSE images showing the lamellar microstructure (a, b) before and (c, d) after exposure at 700°C for 10,000 h in air.

Fig. 2 SEM images showing (a) the normal (SE) and (b) cross sectional view (BSE) of the EDM surface before exposure.

Fig. 3 (a) The normal (SE) and (b-d) cross sectional view (BSE) of the shot peened surface before exposure. The depth of the deformed region is shown in (b) and the barely deformed lamellar packed are arrowed in (c).

Fig. 4 Micro hardness profiles of shot peened specimens under three thermal exposure conditions.

Fig. 5 (a) BSE image showing the electropolished surface before exposure, (b) an SE image showing the smooth surface (arrowed) after electropolishing.

Fig. 6 (a) The normal SE view and (b) cross sectional BSE view of the EDM surface after exposure-oxidation at 700°C for 10000 h. (c) BSE image of the middle part of (b) at a larger magnification showing the diffusion layer.

Fig. 7 (a) The normal SE view, and (b), (c) cross sectional BSE view of the shot peened surface after exposure-oxidation at 700°C for 10000 h. Note that the oxidation scale consists of a loose layer, a grey layer and a white layer, below which is a diffusion layer containing recrystallised equiaxed γ grains.

Fig. 8 (a) EDX spot analyses (spot numbers indicated) on the oxidized shot peening surface after exposure-oxidation at 700°C for 10000 h, (b) the corresponding element profiles across the surface layer, refer to the text for the details, (c) and (d) spectra taken from point 1 and 4, respectively.

Fig. 9 (a) The normal SE view, and (b), (c) cross sectional BSE view of electropolished surface after exposure-oxidation at 700°C for 10000 h. Note that the oxidation scale is ~ 10 μm thick, consisting of a loose layer, a grey layer and a white layer, below which form some equiaxed γ grains.

Fig. 10 S-N fatigue performance of four types of surface in three exposure conditions: (a) no exposure (Group A), (b) block exposure without oxidation (Group B), (c) individual exposure and oxidation (Group C).

Fig. 11 S-N fatigue performance of four types of surface in three exposure groups: (a) EDM, (b) shot peening, (c) electropolishing and (d) V notch (A, B, C denote Group A, B, and C, respectively).

Fig. 12 SEM images from Group A specimens showing the fatigue fracture (a) near the V-notched root, failed at σ_{max}= 176 MPa , 3.24×10^{6} cycles and (b) near the shot peened surface, failed at σ_{max}= 570 MPa, 5×10^{5} cycles).

Table 1 The preparation procedure of the maximum stressed surface for fatigue testing

Surface prepared	Preparation procedure
EDM wire plane-sited	One pass EDM wire to shape
EDM wire V notch (Kt=3)	One pass EDM wire to shape
Shot peening	One pass EDM wire to shape, grinding, shot peening
Electropolishing	One pass EDM wire to shape, grinding and polishing, electropolishing

Table 2 Surface roughness Ra (μm) with error range for each surface and exposure condition.

Specimen (Group)	EDM (A, B)	Shot peening (A, B)	Electropolishing (A, B)	EDM (C)	Shot peening (C)	Electropolishing (C)
Surface roughness Ra (μm)	2.07±0.1	0.63±0.01	0.22±0.01	1.82±0.01	0.67±0.01	0.31±0.01

Table 3 S-N fatigue results and data analysis for EDM, shot peening and electropolishing specimens ($\sigma_{0.2}$=486 MPa before exposure, $\sigma_{0.2}$=477 MPa after exposure).

Exposure Condition (Group)	Specimen surface Condition	σ_{FL} (MPa)	$\sigma_{FL}/\sigma_{0.2}$	Increase in σ_{FL} relative to EDM (%)	Change in σ_{FL} relative to Group A(%)	Change in σ_{FL} relative to Group B(%)
No exposure	EDM wire	380	0.78	—	—	—
(Group A)	Shot peening	550	1.13	45	—	—
	Electronpolishing	480	0.99	26	—	—
Block exposure	EDM wire	400	0.84	—	5	—
(Group B)	Shot peening	635	1.32	59	15	—
	Electronpolishing	615	1.29	54	28	—
Individual exposure	EDM wire	500	1.05	—	32	25
-oxidation	Shot peening	510	1.07	2	-7	-20
(Group C)	Electronpolishing	570	1.19	14	19	-7

Table 4 S-N fatigue results and data analysis for V notch (K_t=3) specimens ($\sigma_{0.2}$=486 MPa before exposure, $\sigma_{0.2}$=477 MPa after exposure)

Exposure condition (Group)	σ_{FL} (MPa)	$\sigma_{FL}/\sigma_{0.2}$	Increase in σ_{FL} relative to Group A(%)	K_f	K_f/K_t	Notch sensitivity factor Q
No exposure (Group A)	146	0.30	—	2.60	0.87	0.80
Block exposure (Group B)	200	0.42	37	2.00	0.67	0.50
Individual exposure-oxidation (Group C)	210	0.44	44	2.38	0.79	0.69

Figure1

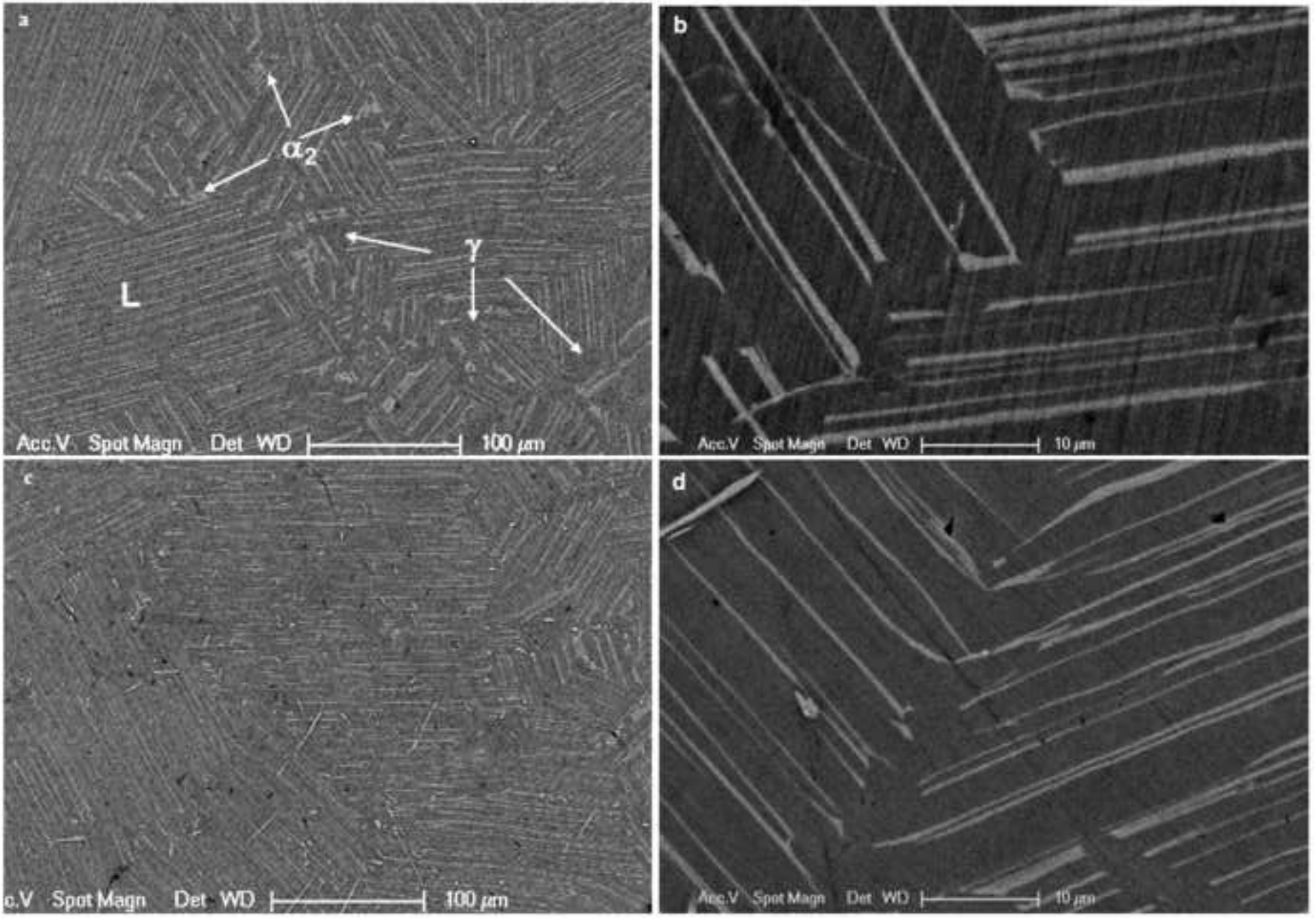

Fig. 1 SEM BSE images showing the lamellar microstructure (a, b) before and (c, d) after exposure at 700°C for 10,000 h in air.

Figure2

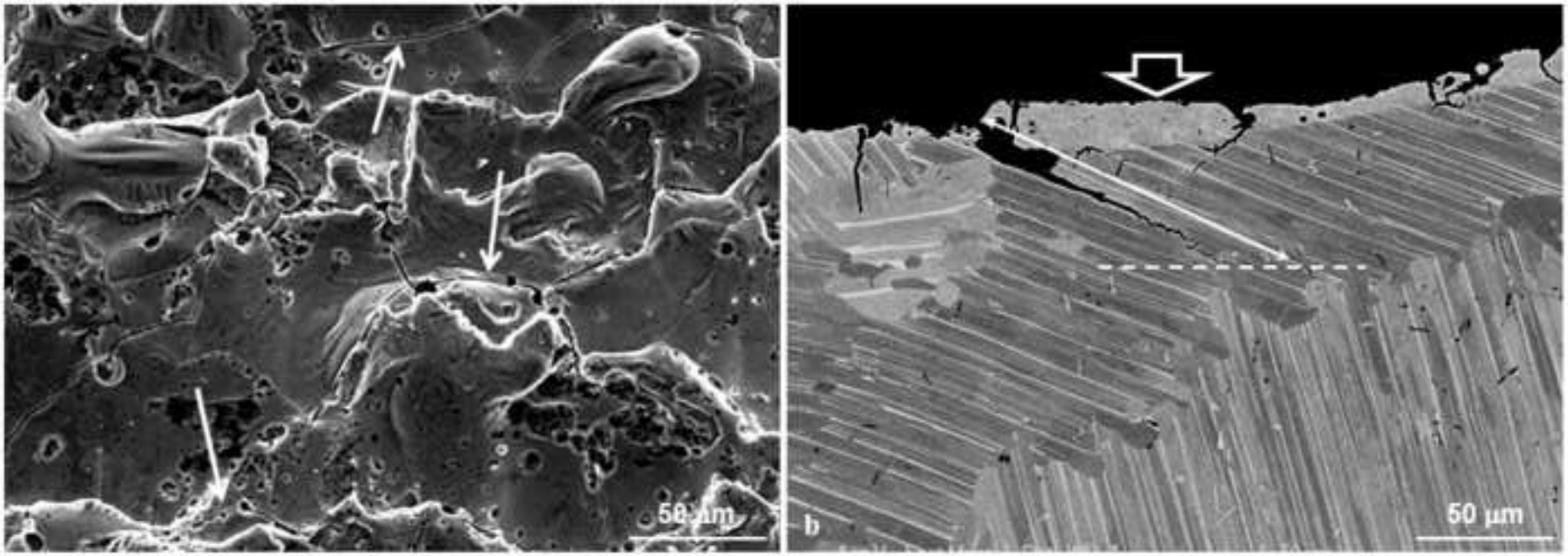

Fig. 2 SEM images showing (a) the normal (SE) and (b) cross sectional view (BSE) of the EDM surface before exposure.

Figure3

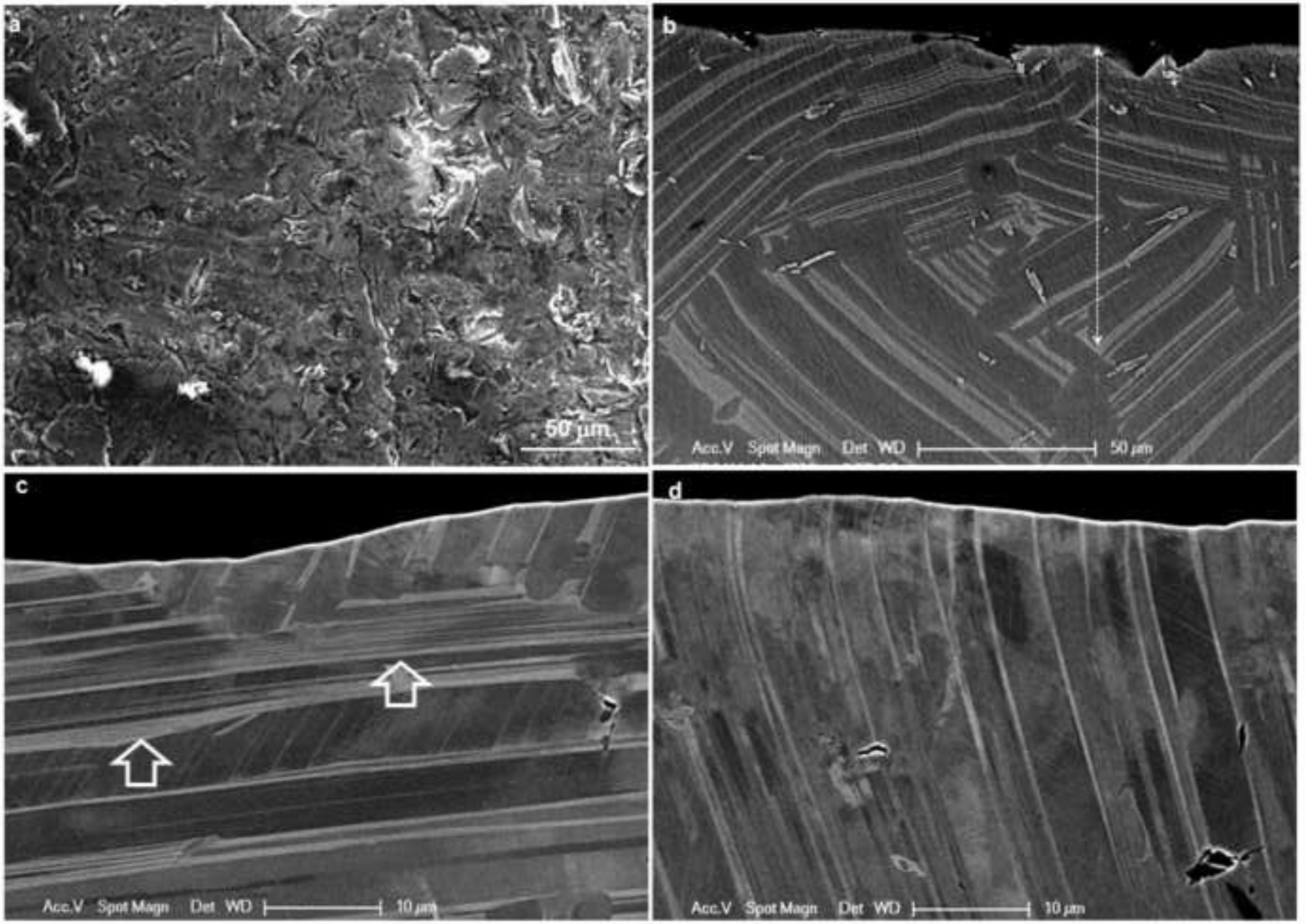

Fig. 3 (a) The normal (SE) and (b-d) cross sectional view (BSE) of the shot peened surface before exposure. The depth of the deformed region is shown in (b) and the barely deformed lamellar packed are arrowed in (c).

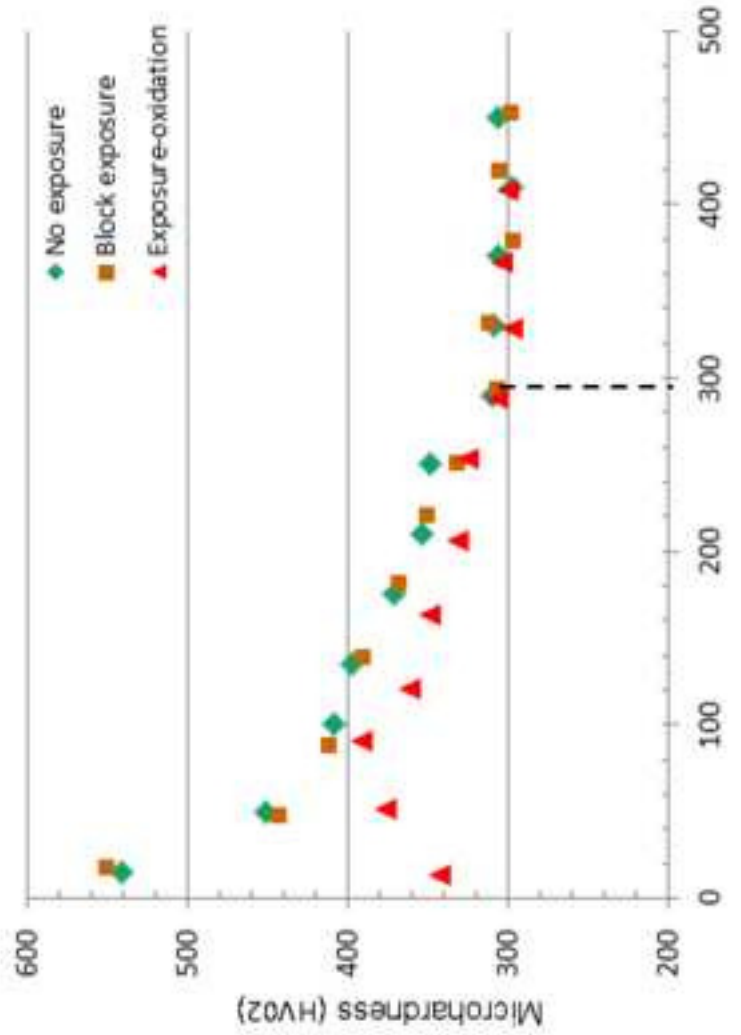

Fig. 4 Micro hardness profiles of shot peened specimens under three thermal exposure conditions.

Figure4

Figure5

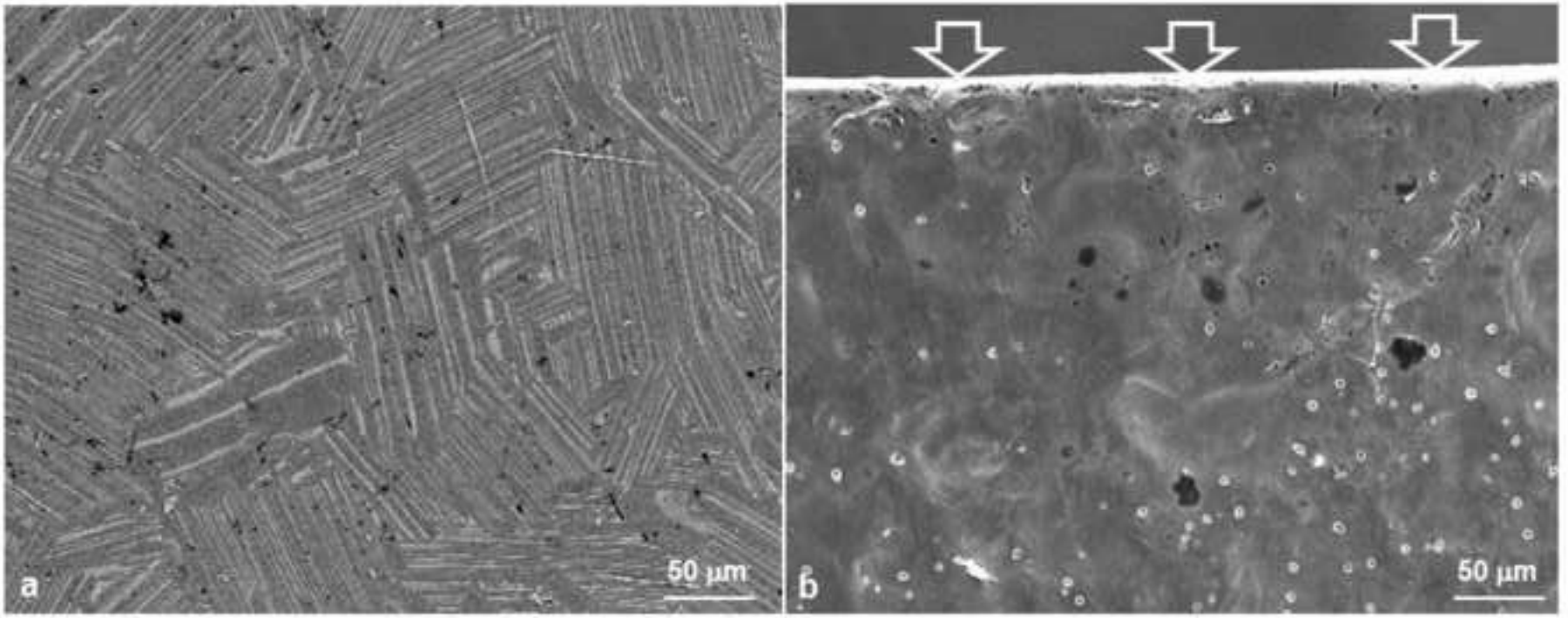

Fig. 5 (a) BSE image showing the electropolished surface before exposure, (b) an SE image showing the smooth surface (arrowed) after electropolishing.

Figure6

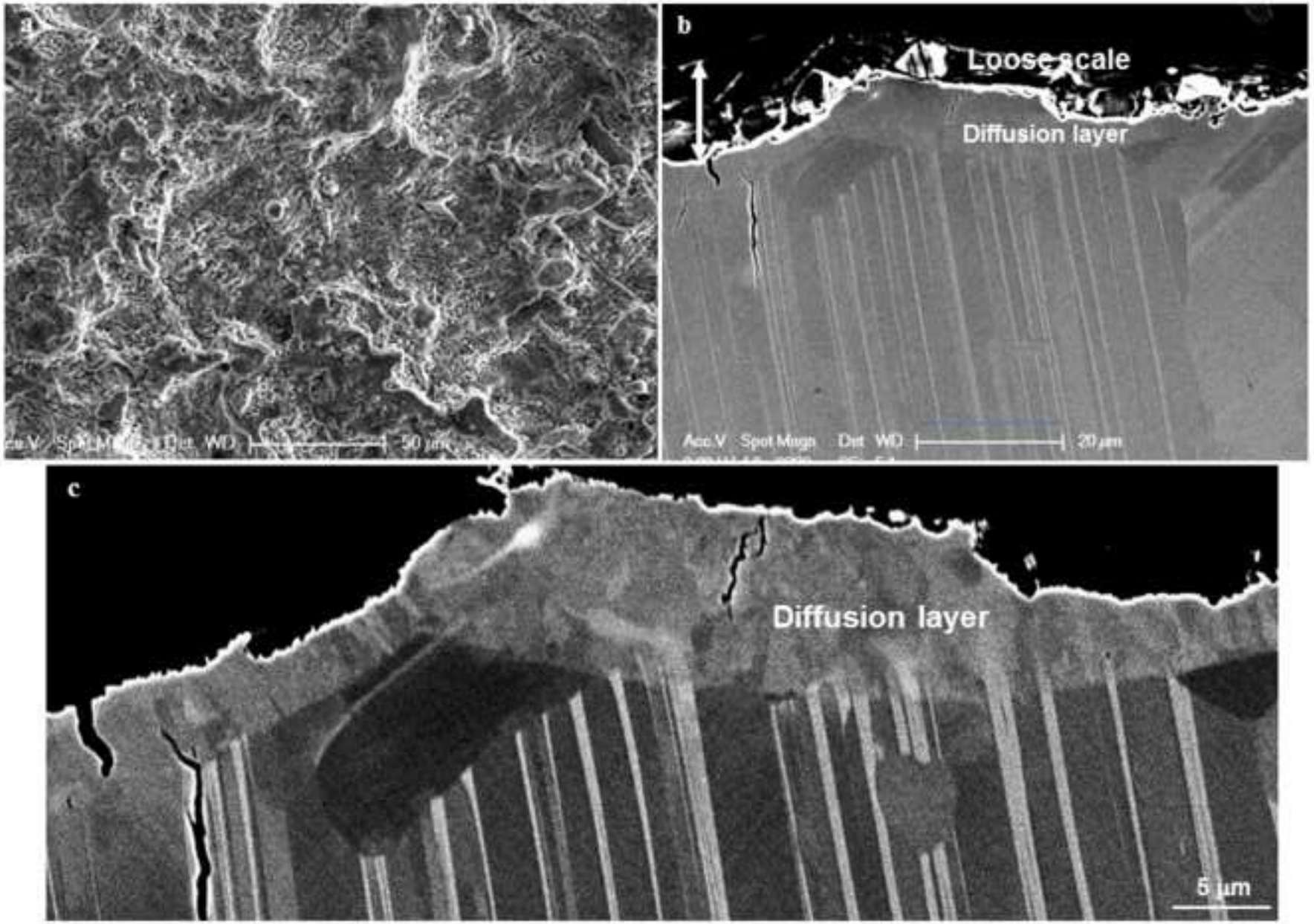

Fig. 6 (a) The normal SE view and (b) cross sectional BSE view of the EDM surface after exposure-oxidation at 700°C for 10000 h. (c) BSE image of the middle part of (b) at a larger magnification showing the diffusion layer.

Figure7

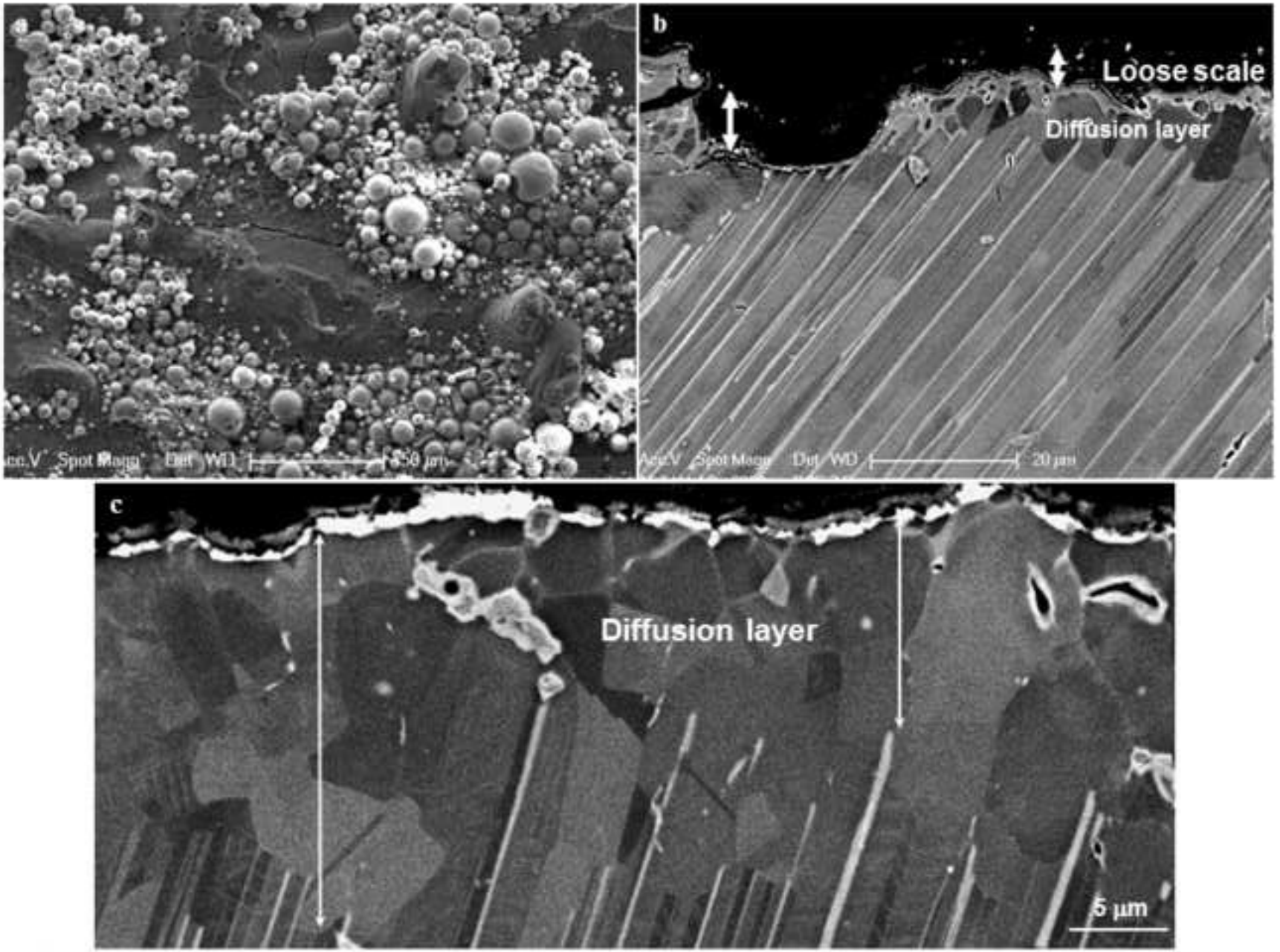

Fig. 7 (a) The normal SE view, and (b), (c) cross sectional BSE view of the shot peened surface after exposure-oxidation at 700°C for 10000 h. Note that the oxidation scale consists of a loose layer, a grey layer and a white layer, below which is a diffusion layer containing recrystallised equiaxed γ grains.

Figure8

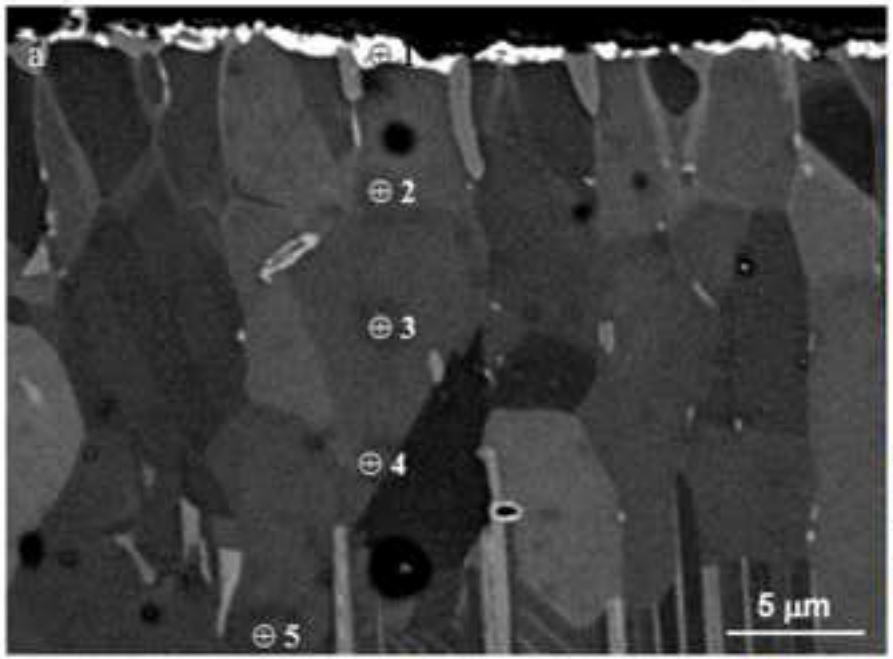

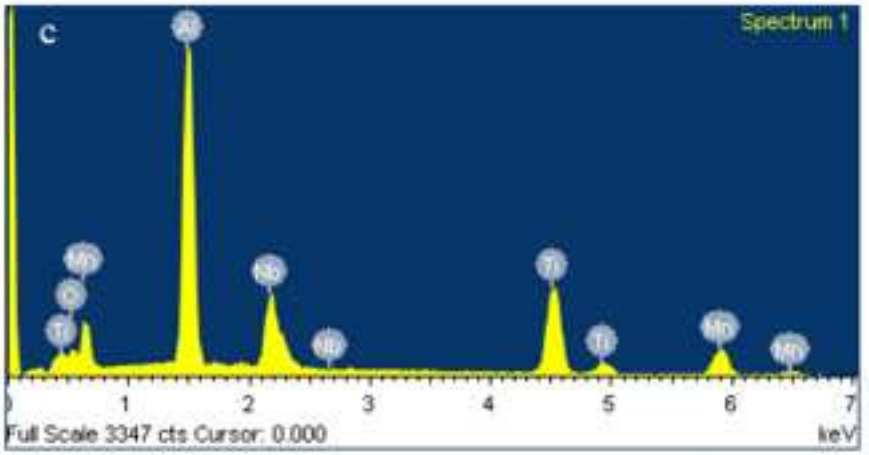

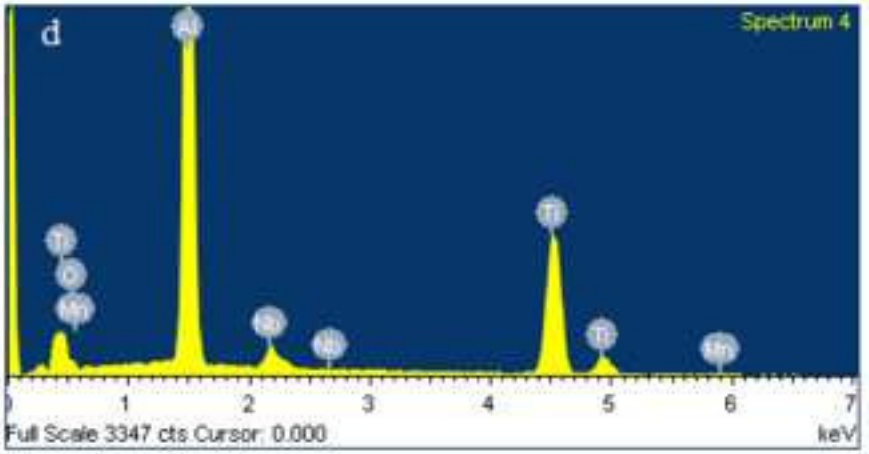

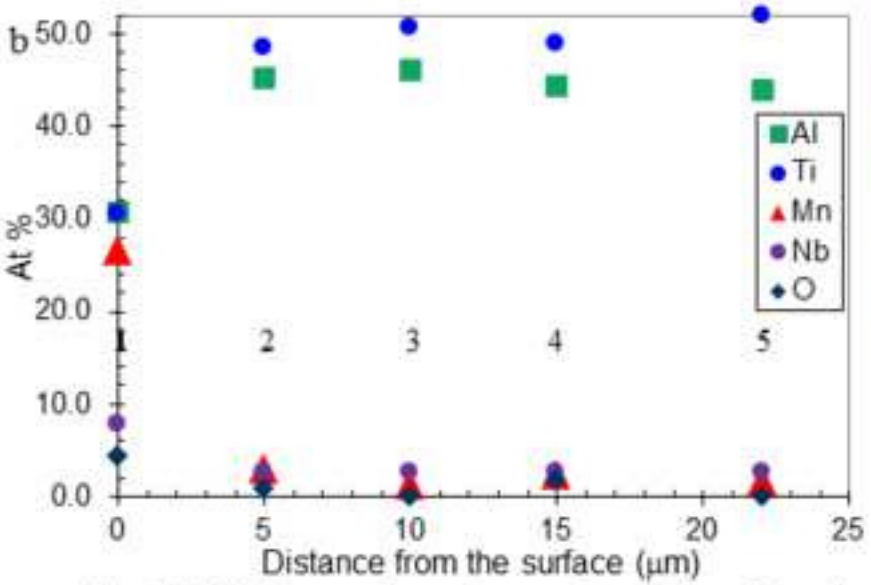

Fig. 8 (a) EDX spot analyses (spot numbers indicated) on the oxidized shot peening surface after exposure-oxidation at 700°C for 10000 h, (b) the corresponding element profiles across the surface layer, refer to the text for the details, (c) and (d) spectra taken from point 1 and 4, respectively.

Figure9

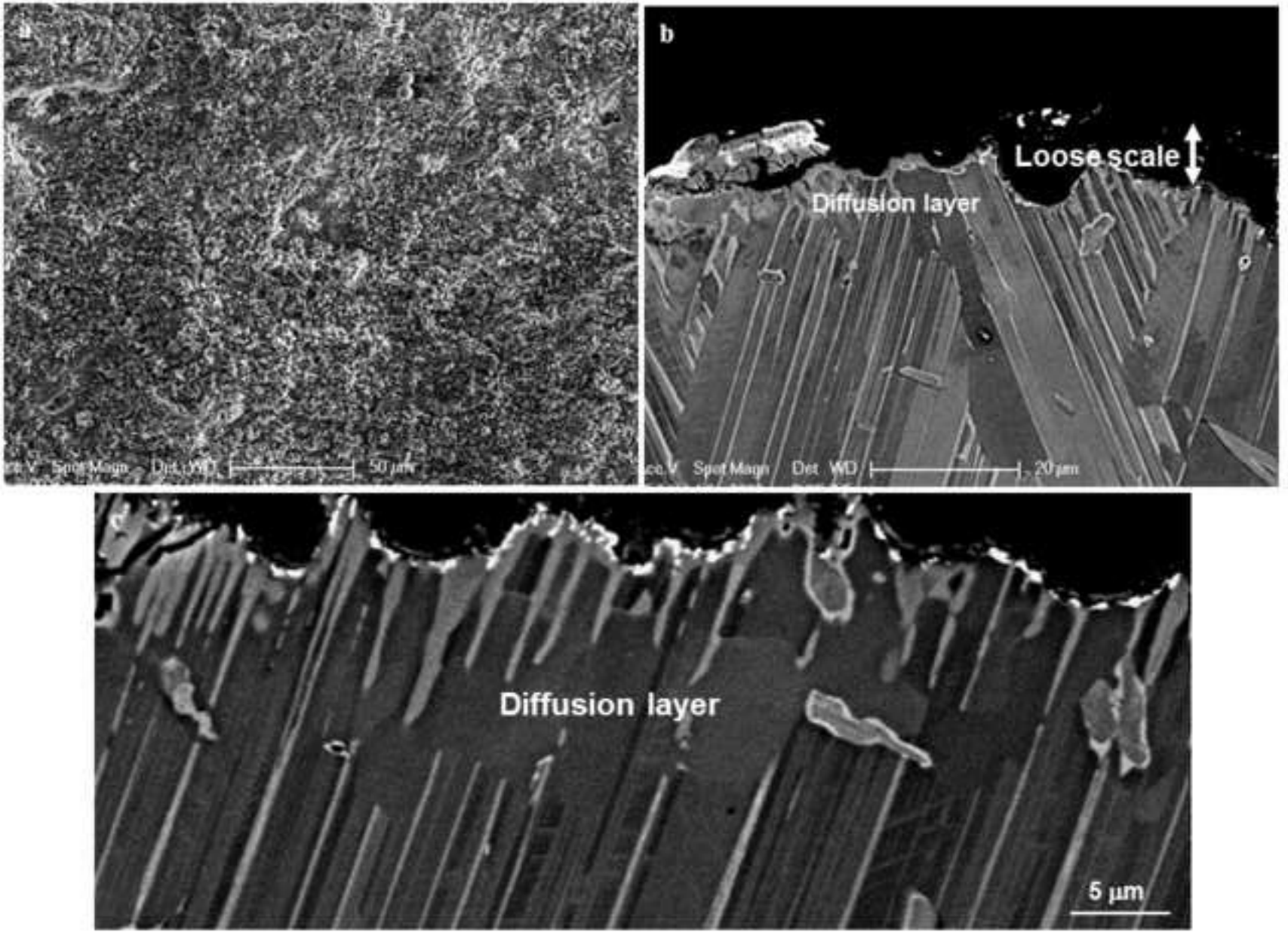

Fig. 9 (a) The normal SE view, and (b), (c) cross sectional BSE view of electropolished surface after exposure-oxidation at 700°C for 10000 h. Note that the oxidation scale is ~ 10 µm thick, consisting of a loose layer, a grey layer and a white layer, below which form some equiaxed γ grains.

Figure10

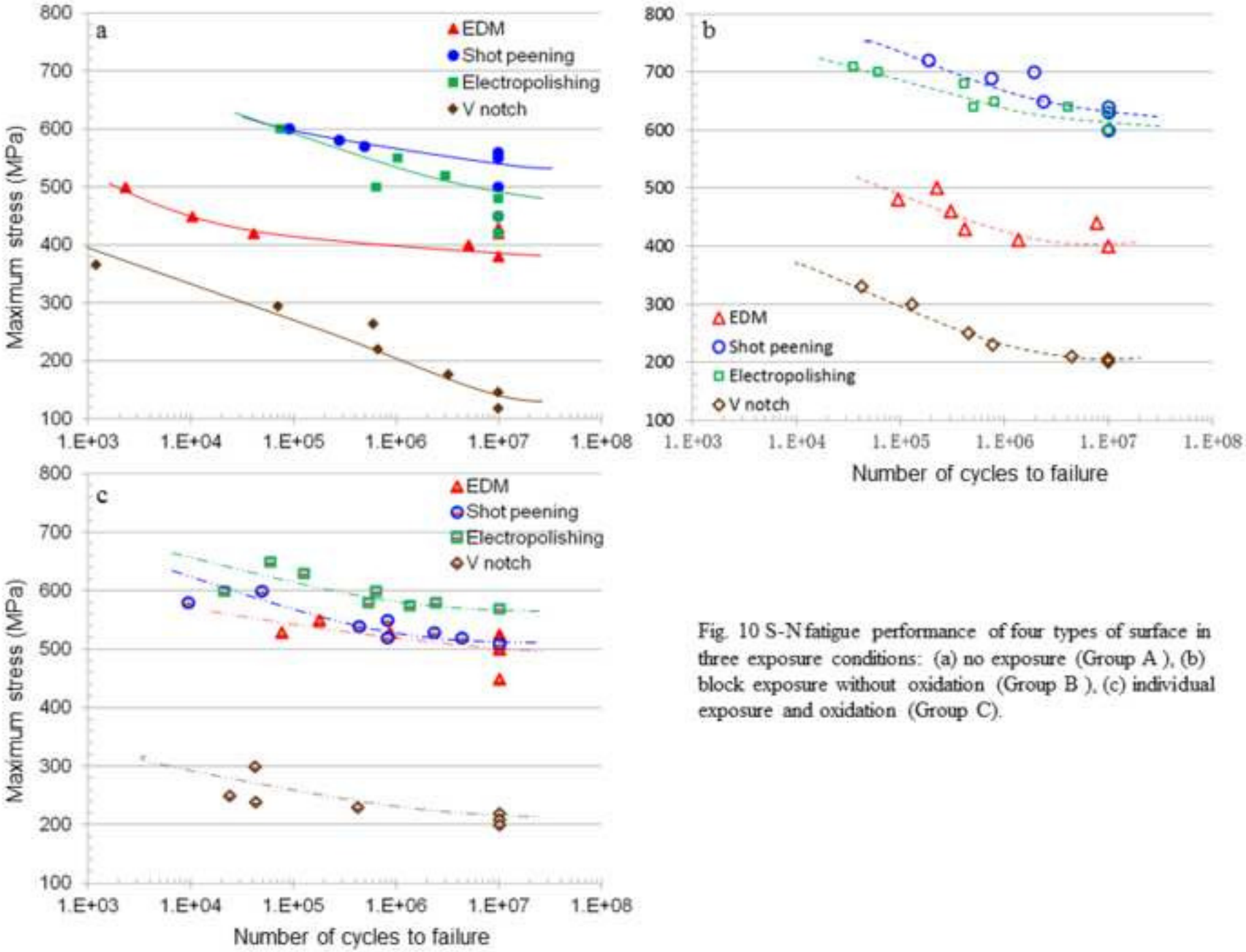

Fig. 10 S-N fatigue performance of four types of surface in three exposure conditions: (a) no exposure (Group A), (b) block exposure without oxidation (Group B), (c) individual exposure and oxidation (Group C).

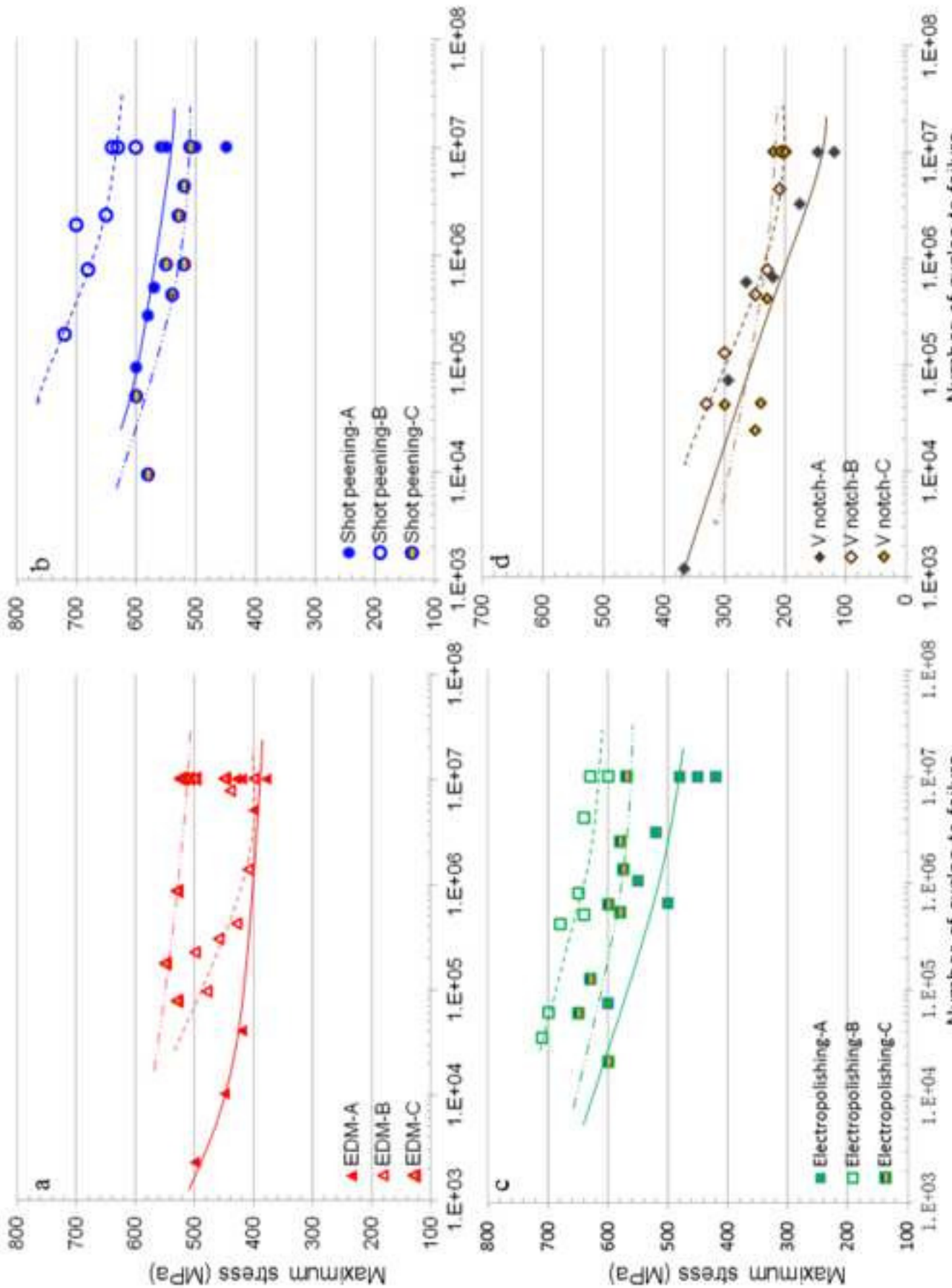

Fig. 11 S-N fatigue performance of four types of surface in three exposure groups: (a) EDM, (b) shot peening, (c) electropolishing and (d) V notch (A, B, C denote Group A, B, and C, respectively).

Figure11

Figure12

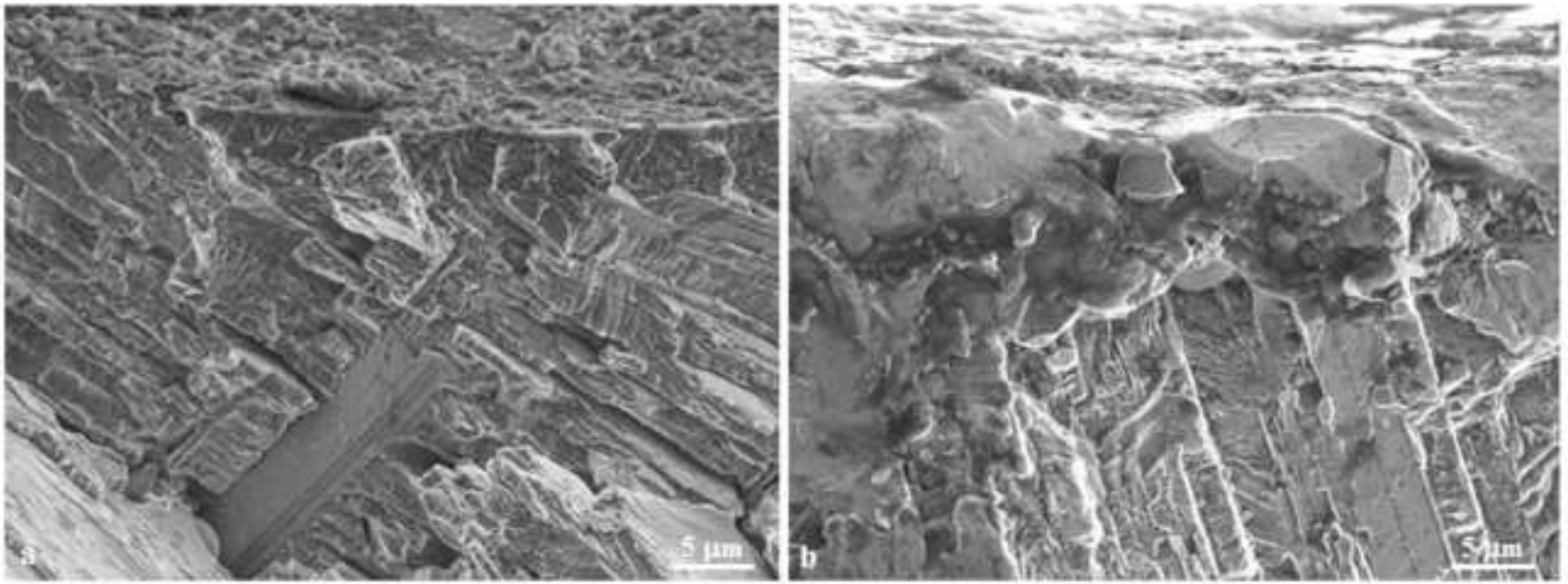

Fig. 12 SEM images from Group A specimens showing the fatigue fracture (a) near the V-notched root, failed at σ_{max}= 176 MPa , 3.24×10^{6} cycles and (b) near the shot peened surface, failed at σ_{max}= 570 MPa, 5×10^{5} cycles) .